Hawking-radiation-ignited autocatalytic formation of primordial black holes

Alexander Yakimenko 1,2

¹Department of Physics, Taras Shevchenko National University of Kyiv, 64/13, Volodymyrska Street, Kyiv 01601, Ukraine ²Dipartimento di Fisica e Astronomia 'Galileo Galilei', Universitá di Padova, via Marzolo 8, 35131 Padova, Italy

We propose and analyze an autocatalytic mechanism in which bursts of Hawking radiation from evaporating micro-primordial black holes (PBHs) trigger the collapse of near-critical plasma overdensities. In a primordial plasma seeded with such patches, this feedback self-organizes into a traveling ignition front that successively forms new PBHs and then self-quenches as the Universe expands. A minimal reaction-diffusion model yields conservative criteria for ignition and freeze-out and predicts a stochastic gravitational-wave background with a sharp causal low-frequency edge set by the freeze-out correlation length and largely insensitive to Planck-scale PBH endpoint microphysics. The resulting sub-Hz-to-audio band and amplitudes satisfy cosmological energy-injection bounds, providing a clean, testable target for forthcoming gravitational-wave observatories.

If dark matter is composed of primordial black holes (PBHs) – a minimal, purely gravitational candidate – it is subject to tight multi-probe constraints from CMB anisotropies, dynamics, accretion, and lensing [1–4]. A robust low-mass bound follows from Hawking radiation (HR) [5]: a black hole of mass M emits thermally at $T_H = (T_{\rm Pl}/8\pi)(M_{\rm Pl}/M)$, so its semiclassical lifetime scales as $\tau \propto M^3$; PBHs with $M \lesssim 10^{14} \,\mathrm{g}$ evaporate by today [6–9], and T_H approaches the Planck scale for $M \sim M_{\rm Pl}$. Quantum backreaction and possible discrete line structure are then expected to modify the emission, making both the spectrum and effective lifetime sensitive to quantum-gravity microphysics [10–12]. A widely discussed possibility is that evaporation terminates in a stable Planck-mass relic (PMR) [2, 3, 13–19], with several independent theoretical motives for such stabilized endpoints [12, 20–27]. Nonemitting relics are compatible with current constraints [2, 16, 28–32], but the key challenge for PMR dark matter is achieving a sufficient relic abundance without violating these bounds. Standard radiation-era collapse ties PBH masses to the horizon at formation; critical collapse broadens but does not break that link [33–36], while other proposed micro-PBH channels invoke enhanced small-scale power, topological defects, or first-order phase transitions [1, 2, 8, 37–39]. By contrast, we introduce a subhorizon, HR-driven ignition mechanism that seeds micro-PBHs without extreme fine—tuning of the primordial initial conditions.

We propose that Hawking bursts from evaporating micro–PBHs can stimulate further PBH formation in the early Universe. A seed population of micro–PBHs $(M_{\rm Pl} < M \ll M_{\odot})$ emits short EM/hadronic bursts whose small mean free paths at early times enable rapid, localized energy deposition in near–threshold regions, transiently reducing pressure support and pushing some patches above the collapse threshold. Because such near–critical regions are parametrically more abundant than the spontaneously collapsing tail, modest localized deposits can substantially enhance the formation rate without extreme tuning of primordial fluctuations [35, 36]. In this PBH–mediated autocatalytic regime, the plasma

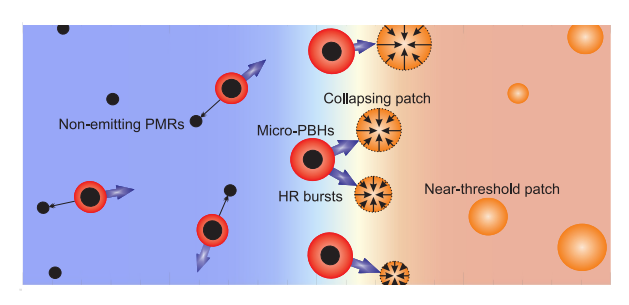
is the fuel, HR acts as the catalyst, and micro-PBHs are the intermediates: newborn micro-PBHs evaporate promptly, their bursts drive further collapses, and the net multiplication is briefly supercritical until expansion and transport weaken deposition, leaving a saturated relic abundance consistent with BBN and CMB energy-injection limits [31, 32]. At the collective level, this ignition admits a minimal reaction-diffusion description of energy-limited conversion of plasma into micro-PBHs; the resulting traveling front forms new PBHs, self-quenches as the Universe expands, and fixes a freezeout scale that imprints a sharp causal low-frequency edge and a finite, nearly flat plateau in the stochastic gravitational-wave spectrum, largely independent of end-point microphysics.

Minimal kinetic model for the ignition phase.— We focus on a short interval $t_0 \leq t \ll H^{-1}$ when the plasma is still dense and contains near—threshold patches that can form new PBHs. On this timescale we work in a small comoving region where expansion is negligible and the plasma is approximately homogeneous.

Let $\rho_r(t)$ be the local plasma energy density available for compaction growth within this control volume (the ignition–accessible reservoir), and let $\rho_{\rm PBH}(t)$ be the energy density in active micro–PBHs (those currently emitting Hawking bursts). Their coarse–grained evolution is

$$\dot{\rho}_{PBH} = -\gamma \,\rho_{PBH} + \alpha \,\rho_{PBH} \,\rho_r + S(\rho_r, t). \tag{1}$$

The first term describes evaporation, with an effective loss rate γ that returns energy to the plasma via HR bursts. The second term, $\alpha \, \rho_{\rm PBH} \rho_r$, describes HR–catalyzed conversion of plasma into new micro–PBHs; α encodes short–mfp EM/hadronic deposition, response time, and near–threshold statistics, and does not describe accretion–driven growth of existing PBHs. The source $S(\rho_r,t)$ accounts for spontaneous (non–catalyzed) PBH production from rare supercritical overdensities; we model it as $S(\rho_r) = \beta \, \rho_r^2$, where β parametrizes the small tail probability in a Gaussian radiation field and is taken constant over the short ignition interval. If a preexisting horizon–scale PBH population is assumed, one may



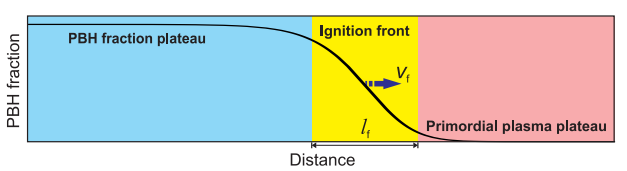


FIG. 1. Schematic of a Hawking–radiation–triggered ignition cascade. Micro–PBHs emit short HR bursts (blue arrows) that deposit energy within a causal patch (orange shell), tipping nearby near-threshold patches to collapse and creating new micro–PBHs, that launch further bursts and finally evaporate to non-emitting PMRs. Bottom: rescaled PBH density across the ignition front, which propagates with speed v_f and has thickness ℓ_f . (Not to scale.)

instead set S=0 during ignition and encode seeding in the initial compact component.

During the brief ignition stage we treat a small comoving region as an active reservoir. HR from PBHs splits into locally deposited EM/hadronic secondaries, which feed this reservoir, and escaping channels (neutrinos, gravitons, long-mfp photons) that do not return to drive collapse; the latter are absorbed into the effective gain and diffusion coefficients and into the finite ignition duration. Over this short interval we approximate the active energy as constant, $\rho_r(t) + \rho_{PBH}(t) \simeq \varepsilon_0$, with only a tiny fraction of the cosmological radiation bath—near threshold patches—participating in ignition, so global depletion is negligible. Within such a patch we set $\rho_r \simeq$ $\varepsilon_0 - \rho_{\rm PBH}$ and reduce the dynamics to a single evolution equation for $\rho_{\rm PBH}$. In the initial regime $\rho_{\rm PBH} \ll \rho_r \simeq \varepsilon_0$ a linearization gives $\dot{\rho}_{\mathrm{PBH}} \simeq (\alpha \, \varepsilon_0 - \gamma) \, \rho_{\mathrm{PBH}} + \beta \, \varepsilon_0^2$. Defining $\varepsilon_{\rm th} = \gamma/\alpha$, any nonzero seed grows if $\varepsilon_0 > \varepsilon_{\rm th}$ (catalyzed gain outpaces evaporation), whereas for $\varepsilon_0 \leqslant \varepsilon_{\rm th}$ active PBHs decay and no ignition occurs. As expansion reduces $\rho_r(t)$ the condition $\lambda = \alpha \rho_r(t) - \gamma \leq 0$ provides a practical freeze-out criterion. Non-emitting PMRsif they exist—appear only after active micro-PBHs have evaporated and therefore do not affect ignition kinetics.

Normalizing $y = \rho_{\mathrm{PBH}}/\varepsilon_0$ gives $\dot{y} = f_{\mathrm{r}}(y)$ with $f_{\mathrm{r}}(y) = \beta \, \varepsilon_0 (1-y)^2 + \alpha \, \varepsilon_0 (1-y) \, y - \gamma \, y = (\beta - \alpha) \, \varepsilon_0 \, (y-y_1) (y-y_2)$, where y is the compact fraction and $y_1 < y_2$ are the real zeros for $0 \le \beta < \alpha$. When the catalytic gain is subcritical $(\lambda < 0)$, quadratic seeding and evaporation balance at a small quasi–steady baseline $y_* \simeq \beta \, \varepsilon_0 / (\gamma - \alpha \, \varepsilon_0)$ for $y \ll 1$. For $\lambda > 0$ any nonzero seed grows; if $\alpha > \beta$, the upper root y_2 is globally attracting on $0 \le y \le 1$ and y_1 is repelling, whereas for $\alpha \le \beta$ stability is reversed

and no self–sustained ignition occurs. Thus λ controls ignition onset and sets freeze–out once dilution drives $\lambda \to 0$, while the nonlinear reaction self–saturates the evolution toward its attractive fixed point. We work in the weak–seeding regime $0 < \beta \ll \alpha$, but the conclusions are unchanged if $\beta = 0$ and seeding is purely initial.

The rescaling $u=(y-y_1)/(y_2-y_1)\in (0,1)$ reduces the dynamics to the logistic form $\dot{u}=r\,u(1-u)$, with mesoscopic growth rate r setting the saturation timescale r^{-1} and $r^2=(\alpha\,\varepsilon_0-\gamma)^2+4\,\gamma\,\beta\,\varepsilon_0$. Having established local ignition and saturation in a homogeneous cell, we next ask how spatial inhomogeneities and effective transport organize ignition into traveling fronts and fix the freezeout correlation length, as illustrated in Fig. 1.

Spatial transport and Fisher-KPP fronts. scribe how ignition organizes in space we now include spatial inhomogeneity and transport. Coarse–graining at mesoscopic scales, $\ell_{\rm mfp} \ll L \ll c/H$ and $t_{\rm dep} \ll t \ll H^{-1}$, makes the dominant spatial coupling effectively diffusive. Here $t_{\rm dep} \sim \mathcal{O}(1-10)\,\ell_{\rm mfp}/c$ is the EM/hadronic deposition time, with $t_{\rm dep} \ll t_{\rm sound} = R/c_s \ll H^{-1}$. This diffusion summarizes two processes distinct from the local reaction rate: (i) short-mfp EM/hadronic cascades from Hawking bursts redistribute energy quasi-locally before full thermalization, inducing a nearest-neighbor, effectively diffusive coupling of the compact fraction (akin to early-Universe energy-deposition kernels in BBN/CMB analyses [40]); and (ii) stochastic recoil from anisotropic Hawking emission drives a random walk of evaporating micro-PBHs [6, 41, 42], which coarse-grains to an additional diffusion channel. We subsume the effective diffusivity D and the logistic reaction term r u(1-u) into the classical Fisher-KPP equation

$$\partial_t u(x,t) = D \,\partial_x^2 u(x,t) + r \,u(x,t) \,\{1 - u(x,t)\}\,,\tag{2}$$

which captures diffusion–limited autocatalytic growth [43, 44]. This reduction to a single reaction–diffusion equation is analogous to standard front–propagation treatments in combustion and population dynamics, where detailed conservation laws are coarse–grained into an effective Fisher–KPP front once a scale separation between a thin active zone and a background reservoir is assumed [43–45].

Equation (2) admits traveling–front solutions $u(x,t) = F(\xi)$, $\xi = x - vt$, with $F(-\infty) = 1$ and $F(+\infty) = 0$. Linearizing the leading edge $(F \ll 1)$ gives $F \sim e^{-k\xi}$ and v(k) = Dk + r/k, minimized at $k_c = \sqrt{r/D}$, so that $v_c = 2\sqrt{Dr}$ and $\ell_f \sim \sqrt{D/r}$. An analytic solution exists for $v_{\text{AZ}} = \frac{5}{2\sqrt{6}}v_c > v_c$ with $F(\xi) = [1 + \exp(\xi\sqrt{r/(6D)})]^{-2}$ [46], while no elementary form is known at $v = v_c$. For ignition–type (steep) initial data the KPP selection principle yields convergence, up to a translation, to the minimal wave [44, 47, 48]. Traveling fronts are nonlinearly stable: pushed $(v > v_c)$ waves relax exponentially, whereas pulled $(v = v_c)$ waves relax algebraically with the Bramson shift [45, 49–51]. To illustrate selection, the inset of Fig. 2 shows a numerical solution of Eq. (2)

started from a steep sigmoid profile with three localized bumps. Small–scale inhomogeneities are smoothed by diffusion and absorbed into the leading edge, so the system rapidly forgets the initial details: a pulled front emerges with asymptotic speed $v \to v_c$ and thickness $\sim \ell_f$. Hence the freeze–out correlation length is mesoscopic: it is set by coarse–grained transport and growth parameters and by the short ignition window, not by the microscopic structure of the seeds.

Ignition viability. – In the standard picture an evaporating PBH produces an outward, high-pressure flash that opposes collapse in the primordial plasma; this is true for free-streaming channels (gravitons, neutrinos) and for spatially homogeneous heating. Here we instead isolate a narrow causal window in which shortmfp EM/hadronic secondaries from Hawking bursts are promptly absorbed and locally raise the inner compaction of near-critical patches. Because collapse thresholds depend on profile as well as amplitude, a small, well-timed local deposit can sharpen the core compaction at fixed $\delta = \delta \rho_r / \rho_r$ and lower the effective threshold [35, 36, 52]. We do not invoke exotic focusing ("BH out of light") or ultra-rare head-on collisions; free-streaming power is treated as noncatalytic, consistent with quantum focusing/inequality bounds that disfavor horizon formation from outgoing radiation [53, 54]. Ignition therefore operates only in a finite PBH mass window: very light micro-PBHs have intense Hawking power but limited total energy and can tip only a modest number of near-threshold patches, whereas very massive PBHs evaporate so slowly that most of their output is released after the plasma has cooled and no longer satisfies the tipping criterion.

Quantitative tipping criterion. - Consider a nearcritical patch with $\delta = \delta_c - \varepsilon$ (0 < ε « 1) at horizon entry. A nearby micro-PBH releases a terminal burst with energy $\Delta E_{\rm burst}$. The short-mfp electromagnetic/hadronic component deposits a temperaturedependent fraction $f_{\text{dep}}(T)$ locally within a causal volume $V_{\rm dep} = 4\pi R^3/3$ over a sub-acoustic time $t_{\rm dep} \ll$ $t_{\rm sound} \sim R/c_s \ (c_s \simeq c/\sqrt{3})$, so pressure cannot respond. The resulting compact load $\chi = f_{\rm dep} \Delta E_{\rm burst} / (\varepsilon \rho_r V_{\rm dep})$ must satisfy $\chi \gtrsim 1$ to tip the patch; i.e., the locally deposited energy must exceed the deficit $\varepsilon \rho_r V_{\rm dep}$ required to reach threshold. Equivalently, in compaction variables the condition reads $\Delta C(R) = (2G/Rc^4) \Delta E_{\rm dep} \gtrsim \Delta C_{\rm req}$ with $\Delta C_{\text{req}} = C_c - C_{\text{max}}(\delta) \simeq (\partial C_{\text{max}}/\partial \delta)_{\delta_c} (\delta_c - \delta) = \kappa \varepsilon$, where C_{max} is the peak Misner–Sharp compaction and $\kappa = \mathcal{O}(1)$ encodes the weak profile/EOS dependence near threshold [34–36]. Here $\Delta E_{\rm dep} = f_{\rm dep} \Delta E_{\rm burst}$ and $R \lesssim$ R_{comp} is the radius that maximizes \mathcal{C} . Only compact, rapid deposition within R_{comp} increases C; short-mfp EM/hadronic channels contribute to $f_{dep}(T)$, whereas free-streaming species (neutrinos, gravitons) deposit negligibly on sub-acoustic times and thus do not tip nearcritical patches [40, 55, 56]. Using $R \sim c_s t_{\rm dep}$ and $\rho_r \propto T^4$ implies $\chi \propto f_{\rm dep} \Delta E_{\rm burst} T^{-4} t_{\rm dep}^{-3}$, i.e., earlier epochs require faster, more local deposition, while shorter $t_{\rm dep}$ significantly increases the tipping effectiveness.

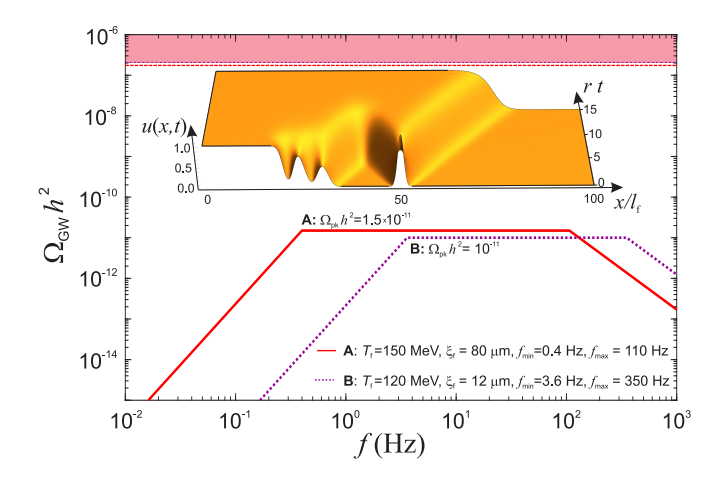


FIG. 2. Stochastic background from HR-ignited fronts: causal f^3 rise, flat plateau of height $h^2\Omega_{\rm pk}$, and UV fall $\propto f^{-2}$. Two benchmark spectra are shown: Case A (solid red) and Case B (dotted blue). Horizontal lines show the CMB-based $\Delta N_{\rm eff}$ cap (A: red dashed; B: blue dotted), and the shaded band marks the excluded region. Inset: Fisher-KPP ignition selects a pulled traveling front. Starting from a steep profile with localized bumps, diffusion and growth erase small-scale structure and the front converges to speed v_c and width ℓ_f .

Quantitatively, the target population is substantial even though PBH formation must remain rare. For a Gaussian field with variance $\sigma^2 \ll \delta_c^2$, the ratio of near–threshold patches in the shell $[\delta_c - \varepsilon, \delta_c]$ to spontaneously supercritical regions $(\delta > \delta_c)$ at the same smoothing scale is $\mathcal{R} = P_{\rm sub}(\varepsilon)/P_{\rm tail} \simeq \varepsilon \delta_c/\sigma^2$. With $\delta_c \in [0.4, 0.5], \ \varepsilon \in [0.02, 0.08], \ {\rm and} \ \sigma \in [0.03, 0.07]$ one finds $1.6 \leqslant \mathcal{R} \leqslant 44$, so tip–able patches can outnumber spontaneous collapses by factors of a few to tens.

Several effects further aid threshold crossing: multiple subcritical deposits can accumulate within one acoustic time before pressure rebound, centrally concentrated loading lowers the effective collapse threshold relative to uniform heating [35, 36], and near the QCD crossover the temporary reduction of c_s^2 and enhanced bulk viscosity promote compaction growth during the first compression [57, 58].

Finally, because a PMR is extremely heavy $(M_{\rm PMR} \simeq M_{\rm Pl})$, its number density is tiny: $n_{\rm PMR,0} \simeq \rho_{\rm DM}/M_{\rm PMR} \sim 10^{-25}\,{\rm cm}^{-3}$ (cosmic mean; spacing $\sim 2000\,{\rm km}$). Even in the local halo with $\rho_{\rm DM} \sim 0.3\,{\rm GeV\,cm}^{-3}$ one finds $n_{\rm PMR} \sim 2.5 \times 10^{-20}\,{\rm cm}^{-3}$ (spacing $\sim 30\,{\rm km}$). PMR production is therefore energy-rather than multiplicity–limited: what matters is the total energy converted into relics, so only a tiny global fraction of the plasma need pass through PMRs during ignition, without requiring many successful collapses per causal region.

SGWB channels during ignition.— The ignition process acts as a broadband GW source by driving overpressured regions whose bulk motion generates time–dependent anisotropic stress. The resulting stochastic background can receive power from expanding fronts

around igniting PBHs, acoustic post–shock sound waves, and a later turbulent tail [59–62]; ignition–induced inhomogeneities can also source a second–order (scalar–induced) background [16, 63], while direct Hawking gravitons yield an ultra–high–frequency, nearly thermal component [64]. In what follows we focus on the lower–frequency environmental signal from ignition–driven flows, whose edge–plus–plateau structure is set by the freeze–out correlation length.

The ignition stage excites mesoscopic bulk flows during a brief active interval and then shuts off. The ignition stage excites a Fisher–KPP front of width ℓ_f and speed v_c (see Fig. 2), so propagation during the active interval $\Delta t_{\rm ign}$ leaves a freeze–out correlation length $\xi_f \simeq \max(\ell_f, v_c \Delta t_{\rm ign})$ and a source coherence scale $\ell_{\rm cut} = \max(\ell_f, \ell_{\rm micro})$, where $\ell_{\rm micro}$ is the short–mean–free–path EM/hadronic deposition footprint and c_s is the sound speed; the associated coherence time satisfies $\tau_{\rm coh} \sim \ell_{\rm cut}/c_s$.

Defining the redshift factor $\zeta_f = a_f/a_0$, a finite correlation length ξ_f fixes the causal low-frequency edge $f_{\min,0} = \zeta_f c/(2\pi \xi_f)$ and implies the standard causal rise $\Omega_{\rm GW} \propto f^3$ for $f \lesssim f_{\rm min,0}$ [61, 65]. Here $\Omega_{\rm GW}(f) =$ $\rho_c^{-1} d\rho_{\rm GW}/d \ln f$ with $\rho_c = 3H_0^2/(8\pi G)$ the critical density. For frequencies $f_{\min,0} \lesssim f \lesssim f_{\max,0}$, with $f_{\max,0} =$ $\zeta_f c_s/(2\pi \ell_{\rm cut})$, the source is short–correlated in time (correlation time $\tau_{\rm coh}$), so its unequal-time correlator is effectively white over the band of interest. Spatial correlations decay over ξ_f , and for modes $k \lesssim \xi_f^{-1}$ the equaltime power spectrum of the anisotropic stress is approximately k-independent, so different correlation volumes add incoherently. The convolution with the GW Green's function then produces a broad maximum with weak scale dependence, which we approximate as a flat plateau $\Omega_{\rm GW}(f) \simeq \Omega_{\rm pk}$ for $f_{{\rm min},0} \lesssim f \lesssim f_{{\rm max},0}$. At higher frequencies $f \gtrsim f_{{\rm max},0}$ the finite coherence time and length suppress the source on small scales, leading to a decaying UV tail that we model as $\Omega_{\rm GW} \propto f^{-p}$ with p a free index; values $p \geq 2$ are motivated by analytic estimates and simulations of short-lived, causal sources such as phase transitions, turbulence, and primordial magnetic fields [60–62, 66–68].

The two spectra in Fig. 2 are drawn from the interior of a conservative mesoscopic domain defined by $\ell_f \geq \ell_{\text{micro}}$, subsonic propagation $v_c \leq c_s$, and strong local absorption $D \ll c_s \ell_{\text{micro}}$. These choices ensure that the ignition front operates within the microphysical window identified earlier from the tipping parameter $\chi \gtrsim 1$, with r and D large enough to form a front on timescales $\ll H^{-1}$ yet small enough to remain compatible with cosmological energy-injection bounds. In both benchmarks $\ell_f > \ell_{\text{micro}}$, so the coherence scale is set by the front, $\ell_{\text{cut}} = \ell_f$, and $f_{\text{min},0}$ and $f_{\text{max},0}$ follow directly from $\xi_f = v_c \Delta t_{\text{ign}}$ and ℓ_f as above. Thus, for given (ξ_f, ℓ_f) (as in Fig. 2) the brokenpower–law template is fixed up to the plateau height Ω_{pk} and the UV index p.

For each benchmark we adopt a conservative plateau normalization $h^2\Omega_{\rm pk}$ that encodes the (unknown) GW conversion efficiency of the ignition stage via $\Omega_{\rm pk} \sim \epsilon_{\rm GW}\,\Omega_{\rm kin}$, where $\Omega_{\rm kin}$ is the bulk–flow energy fraction. A first–principles normalization would require fully coupled relativistic radiation–hydrodynamics with kinetic transport of EM/hadronic cascades and Planck–scale endpoint physics, which lies beyond this proof–of–concept study. Instead, we calibrate $\epsilon_{\rm GW}$ using a well–studied class of short–lived relativistic fluid sources—sound waves from first–order phase transitions—where simulations and analytic templates yield $h^2\Omega_{\rm pk} \sim 10^{-12}$ – 10^{-9} for temporally short, subsonic sources [60, 68–70]. Our benchmark $h^2\Omega_{\rm pk} \sim 10^{-11}$ is therefore conservative for a generic short–lasting plasma source with similar correlation scales and remains well below the $\Delta N_{\rm eff}$ cap.

We translate the standard extra-radiation constraint into a GW integral bound using the relation between $\Delta N_{\rm eff}$ and the integrated GW density [32, 61], $\int d \ln f \, h^2 \Omega_{\text{GW}}(f) \leq 5.6 \times 10^{-6} \, \Delta N_{\text{eff}}, \text{ where } h =$ $H_0/(100\,\mathrm{km\,s^{-1}\,Mpc^{-1}})$. For the broken–power–law template above this integral evaluates to $h^2\Omega_{\rm pk}I$ with I= $1/3+\ln(f_{\rm max,0}/f_{\rm min,0})+1/p,$ so the plateau height is capped at $h^2\Omega_{\rm pk}^{\rm max}=5.6\times10^{-6}\Delta N_{\rm eff}^{\rm max}/I.$ In our benchmarks we adopt p=2 when evaluating I, consistent with UV slopes found for short-lived, causal sources and conservative for the $\Delta N_{\rm eff}$ bound: for fixed $\Omega_{\rm pk}$, larger p would only decrease I and thus weaken the constraint. In Fig. 2 we draw, for each benchmark, a horizontal cap at $h^2\Omega_{\rm pk}^{\rm max}$ (we use a CMB-based $\Delta N_{\rm eff}^{\rm max}=0.2$). This cap applies only to the decoupled GW component. At the epoch of interest, $T \sim 50-150$ MeV, neutrinos remain tightly coupled on Hubble times and thus do not yet contribute to $\Delta N_{\rm eff}$. If ignition persisted past neutrino decoupling, any late power injected into free-streaming neutrinos would enter $\Delta N_{\rm eff}$ and further tighten the radiation budget.

Conclusions. – Hawking-radiation-driven can operate briefly but efficiently in the radiation era, amplifying near-critical collapses while the plasma is dense and then self-quenching as dilution shuts off the gain. This scenario predicts a robust stochastic gravitational-wave background with a sharp causal low-frequency edge set by the freeze-out correlation length—the primary observable—largely insensitive to the unknown Planck-scale evaporation microphysics, so that the edge-plus-plateau spectrum persists even if all micro-PBHs fully evaporate. If evaporation halts at the Planck scale, the same ignition epoch could also yield a population of Planck-mass relics as a purely gravitational dark-matter candidate. Thus the ignition mechanism provides an independently testable route to PBH formation, and its GW signature offers a rare mesoscopic window on early-Universe microphysics.

Acknowledgments. – Valuable discussions with Oleksandr Sobol and Luca Salasnich are gratefully acknowledged.

- B. Carr, K. Kohri, Y. Sendouda, and J. Yokoyama, Reports on Progress in Physics 84, 116902 (2021).
- [2] B. Carr and F. Kühnel, Annual Review of Nuclear and Particle Science 70, 355 (2020), arXiv:2006.02838 [astroph.CO].
- [3] B. Carr and F. Kuhnel, SciPost Phys. Lect. Notes , 48 (2022).
- [4] M. Y. Khlopov, Research in Astronomy and Astrophysics 10, 495 (2010), arXiv:0801.0116 [astro-ph].
- S. W. Hawking, Commun. Math. Phys. 43, 199 (1975).
- [6] D. N. Page, Phys. Rev. D 13, 198 (1976).
- [7] B. J. Carr, K. Kohri, Y. Sendouda, and J. Yokoyama, Phys. Rev. D 81, 104019 (2010).
- [8] A. M. Green and B. J. Kavanagh, J. Phys. G: Nucl. Part. Phys. 48, 043001 (2021).
- [9] B. Carr, F. Kühnel, and M. Sandstad, Phys. Rev. D 94, 083504 (2016).
- [10] M. K. Parikh and F. Wilczek, Phys. Rev. Lett. 85, 5042 (2000).
- [11] M. Arzano, A. J. M. Medved, and E. C. Vagenas, Journal of High Energy Physics 2005, 037 (2005).
- [12] J. D. Bekenstein and V. F. Mukhanov, Phys. Lett. B 360, 7 (1995).
- [13] P. Chen, New Astronomy Reviews 49, 233 (2005).
- [14] J. Maldacena, Journal of High Energy Physics 2021, 79 (2021).
- [15] J. A. de Freitas Pacheco, Universe 4, 62 (2018).
- [16] G. Domènech and M. Sasaki, Class. Quantum Grav. 40, 175007 (2023).
- [17] P. C. W. Davies, D. A. Easson, and P. B. Levin, Physical Review D 111, 103512 (2025).
- [18] M. Calzà, D. Pedrotti, and S. Vagnozzi, Phys. Rev. D 111, 024009 (2025).
- [19] M. Calzà, D. Pedrotti, and S. Vagnozzi, Phys. Rev. D 111, 024010 (2025).
- [20] J. D. Bekenstein, Lettere al Nuovo Cimento 11, 467 (1974).
- [21] R. J. Adler, P. Chen, and D. I. Santiago, Gen. Relativ. Gravit. 33, 2101 (2001).
- [22] S. A. Hayward, Phys. Rev. Lett. 96, 031103 (2006).
- [23] I. Dymnikova, Gen. Relativ. Gravit. 24, 235 (1992).
- [24] P. O. Mazur and E. Mottola, Proc. Natl. Acad. Sci. USA 101, 9545 (2004).
- [25] B. Holdom and J. Ren, Phys. Rev. D 95, 084034 (2017).
- [26] U. Aydemir, J. F. Donoghue, and F. Piazza, Phys. Rev. D 102, 024058 (2020).
- [27] C. Rovelli and F. Vidotto, Phys. Rev. D 90, 127503 (2014).
- [28] J. H. MacGibbon, Nature 329, 308 (1987).
- [29] A. Barrau, C. Rovelli, and F. Vidotto, Phys. Rev. D 100, 123505 (2019).
- [30] X. Calmet and R. Casadio, Eur. Phys. J. C 81, 132 (2021).
- [31] S. K. Acharya and R. Khatri, JCAP **2020** (6), 018.
- [32] Planck Collaboration, Astronomy and Astrophysics 641, A6 (2020), arXiv:1807.06209 [astro-ph.CO].
- [33] M. Shibata and M. Sasaki, Phys. Rev. D 60, 084002 (1999).
- [34] T. Harada, C.-M. Yoo, and K. Kohri, Phys. Rev. D 88, 084051 (2013), arXiv:1309.4201 [astro-ph.CO].
- [35] I. Musco, Phys. Rev. D **100**, 123524 (2019).

- [36] J. C. Niemeyer and K. Jedamzik, Phys. Rev. Lett. 80, 5481 (1998).
- [37] S. Clesse and J. García-Bellido, Phys. Rev. D 92, 023524 (2015).
- [38] S. Clesse and J. Garcia-Bellido, Phys. Dark Univ. 22, 137 (2018), arXiv:1711.10458.
- [39] M. Sasaki, T. Suyama, T. Tanaka, and S. Yokoyama, Class. Quantum Grav. 35, 063001 (2018).
- [40] T. R. Slatyer, Phys. Rev. D 93, 023521 (2016).
- [41] A. Arbey and J. Auffinger, JCAP **2019** (10), 037.
- [42] J. Auffinger and A. Arbey, Comput. Phys. Commun. 264, 107928 (2021).
- [43] R. A. Fisher, Annals of Eugenics 7, 355 (1937).
- [44] A. N. Kolmogorov, I. G. Petrovsky, and N. S. Piskunov, Bull. Univ. Moscow, Ser. A: Math. Mech. 1, 1 (1937).
- [45] U. Ebert and W. van Saarloos, Physica D 146, 1 (2000).
- [46] M. J. Ablowitz and A. Zeppetella, Bulletin of Mathematical Biology 41, 835 (1979).
- [47] D. G. Aronson and H. F. Weinberger, Advances in Mathematics 30, 33 (1978).
- [48] M. Bramson, Memoirs of the American Mathematical Society 44, 0 (1983).
- [49] D. H. Sattinger, Advances in Mathematics 22, 312 (1976).
- [50] P. C. Fife and J. B. McLeod, Archive for Rational Mechanics and Analysis 65, 335 (1977).
- [51] M. Avery and A. Scheel, SIAM Journal on Mathematical Analysis 53, 2206 (2021).
- [52] I. Musco, V. De Luca, G. Franciolini, and A. Riotto, Phys. Rev. D 103, 063538 (2021).
- [53] R. Bousso, Z. Fisher, S. Leichenauer, and A. C. Wall, Phys. Rev. D 93, 064044 (2016).
- [54] L. H. Ford, M. J. Pfenning, and T. A. Roman, Phys. Rev. D 57, 4839 (1998).
- [55] V. Poulin, J. Lesgourgues, and P. D. Serpico, JCAP 2017(3), 043, arXiv:1610.10051 [astro-ph.CO].
- [56] S. Bashinsky and U. Seljak, Phys. Rev. D 69, 083002 (2004).
- [57] F. Karsch, D. Kharzeev, and K. Tuchin, Physics Letters B 663, 217 (2008), arXiv:0711.0914 [hep-ph].
- [58] H. B. Meyer, Physical Review D 76, 101701 (2007).
- [59] S. J. Huber and T. Konstandin, Journal of Cosmology and Astroparticle Physics 2008 (09), 022.
- [60] M. Hindmarsh, S. J. Huber, K. Rummukainen, and D. J. Weir, Physical Review D 96, 103520 (2017).
- [61] C. Caprini and D. G. Figueroa, Classical and Quantum Gravity 35, 163001 (2018).
- [62] C. Caprini, R. Durrer, and G. Servant, JCAP 2009 (12), 024
- [63] K. Kohri and T. Terada, Phys. Rev. D 97, 123532 (2018).
- [64] J. H. MacGibbon and B. R. Webber, Phys. Rev. D 41, 3052 (1990).
- [65] R. Durrer and C. Caprini, Journal of Cosmology and Astroparticle Physics 2003 (11), 010, arXiv:astroph/0305059.
- [66] C. Caprini, R. Durrer, T. Konstandin, and G. Servant, Phys. Rev. D 79, 083519 (2009).
- [67] C. Caprini and R. Durrer, Phys. Rev. D 65, 023517 (2002).
- [68] D. J. Weir, Philosophical Transactions of the Royal Society A 376, 20170126 (2018).

- [69] M. Hindmarsh, S. J. Huber, K. Rummukainen, and D. J. Weir, Phys. Rev. Lett. 112, 041301 (2014).
- [70] C. Caprini, M. Hindmarsh, S. J. Huber, T. Konstandin, J. Kozaczuk, G. Nardini, K. Rummukainen, P. Schwaller,
- A. Tevzadze, and D. J. Weir, JCAP 2016 (04), 001.